Impact of tropospheric anomalies on GBAS integrity

Yuanyuan Zhuang, Zhipeng Wang, Kun Fang, Yanbo Zhu, Beihang University, China

BIOGRAPHY (IES)

Zhipeng Wang received his B.S. degree in communication engineering from the School of Electronics Information & Engineering, Northwestern Polytechnical University (NWPU) in 2006 and received his Ph.D. in traffic information engineering from the School of Electronic Information Engineering, Beihang University in 2013. He is currently an Associate Professor in the School of Electronic Information Engineering, Beihang University. His research focuses algorithms for the combination of ground-based augmentation systems (GBAS) and satellite-based augmentation systems (SBAS), as well as for advanced receiver autonomous integrity monitoring (ARAIM).

Yuanyuan Zhuang received her B.S. degree from Ludong University in 2018. She is currently a graduate student in the National Key Laboratory of CNS/ATM at Beihang University. Her major research interests are ground-based augmentation systems (GBAS), tropospheric characteristics and tropospheric anomaly monitoring for GBAS.

Kun Fang received his Ph.D. degree in traffic information engineering from the School of Electronic Information Engineering, Beihang University in 2017. He is currently a postdoctoral researcher in the School of Electronic Information Engineering, Beihang University. His research focuses on the integrity monitoring and evaluation of a ground-based augmentation systems.

Yanbo Zhu received his B.S. and M.S. degrees from the School of Electronic Information Engineering, Beihang University, in 1992 and 1993, respectively. He is currently a Ph.D. candidate at the School of Electronic Information Engineering, Beihang University and is a Chief Engineer for CNS/ATM Labs and CAAC. His main research interests are air traffic management, aeronautical telecommunication networks, satellite navigation and automatic dependent surveillance.

ABSTRACT

Ground-based augmentation systems (GBAS) improve the positioning accuracy of aircraft through differential correction techniques during the approach process and enable aircraft to achieve higher services through various monitoring algorithms. Many errors need to be eliminated during navigation. Tropospheric delay is one of the most critical errors in a GBAS.

Under normal atmospheric conditions, most of the tropospheric delays can be eliminated by using the difference method and TC model. However, these methods are not applicable under anomalous atmospheric conditions, and abnormal atmospheric conditions have been observed by both the International Civil Aviation Organization (ICAO) and Single European Sky Air Traffic Management Research (SESAR). Anomalous atmospheric conditions pose a great threat to aircraft safety. An integrity monitoring approach may be taken, or the threat may be incorporated into the normal model and overbounded by the protection levels. This paper focuses on non-nominal anomalies in different regions and in different seasons. We found that the maximum residual tropospheric delay caused by non-nominal anomalies exceeds 35 cm. In addition, the frequency of and the maximum residual tropospheric delay caused by the simultaneous occurrence of duct anomalies and non-nominal anomalies are studied here. We found that the maximum frequency of non-nominal and duct anomalies occurring simultaneously exceeds 70%. Finally, this paper used the previously developed overbound method to overbound the two kinds of tropospheric anomalies using data from Dongying Airport. We found that the impact of duct anomalies on the protection levels is greater than that of non-nominal anomalies at Dongying Airport.

1. INTRODUCTION

A GBAS is a system that improves the positioning accuracy of the aircraft through the differential correction technique during the approach process and enables the aircraft to achieve higher services through various monitoring algorithms. To ensure aircraft approach safety, several challenges must be solved, such as the ephemeris error, ionospheric delay, tropospheric delay, multipath and noise. Tropospheric delay is one of the most critical errors for GBAS. For GBAS Approach Service Type (GAST)-D/E/F, a dual-frequency method is proposed to eliminate ionospheric delay and monitor ionospheric gradient anomalies. To meet the stringent requirements of CAT II/III precision approach operations, the troposphere becomes a key factor affecting GBAS security. The main factor affecting tropospheric delay is the atmospheric condition. Under normal atmospheric conditions, aircraft and GBAS stations are subject to similar atmospheric conditions, and tropospheric delays can be eliminated by differential methods. The tropospheric delay between an airplane and GBAS station can be eliminated by the TC model [1]. However, under abnormal atmospheric conditions, tropospheric delays cannot be eliminated by differential methods, and the TC model proposed above is not applicable. The handling of abnormal atmospheric conditions in the current standard documents has not been clearly defined. No monitor has been designed to detect the presence of such abnormal atmospheric conditions.

Research has shown that residual zenith tropospheric delay due to abnormal atmospheric conditions will cause a centimeter-level error, which poses a great threat to aircraft safety. The impact of anomalous atmospheric conditions on GBAS safety needs to be analyzed. Abnormal atmospheric conditions have been observed [2][3]. It is important to evaluate their effects on GBAS safety design and protect an aircraft from these biases. GBAS integrity means that when the positioning information provided by the GBAS system cannot meet the aircraft approach requirements, the system can raise the alarm in time. Abnormal atmospheric conditions are a threat for GBAS; an integrity monitoring approach may be taken, or the threat may be incorporated into the normal model and overbounded by the protection levels. Currently, the differential range standard deviation terms apply to normal atmospheric conditions. Under abnormal atmospheric conditions , the differential range standard deviation terms must be modified to ensure aircraft safety.

There are two possible threats related to the troposphere: non-nominal anomalies, which occur in the horizontal direction, and duct anomalies, which occur in the vertical direction. Non-nominal anomalies are mainly caused by atmospheric phenomena, such as weather fronts and heavy rainfall, which cause the atmospheric conditions experienced by satellite signals arriving at ground stations to differ from the atmospheric conditions experienced by satellite signals arriving at the aircraft [4]. In 2007, Jidong Huang established a weather wall model to simulate non-nominal anomalies [5]. In 2016, Beihang University statistically analyzed the 2015 and 2016 China regional IGS and iGMAS data and established a model for residual tropospheric delay caused by non-nominal anomalies with elevation changes [6]. In 2019, Takayuki Yoshihara observed that the maximum tropospheric spatial gradient in the oblique direction was 87 mm/km [7]. Duct anomalies appear mainly because the TC model is only an estimate of the tropospheric delay, and there are some differences from the actual tropospheric delay; the model is not adapted to atmospheric conditions such as temperature inversion, evaporation ducts, air subsidence and air advection. Due to the different atmospheric conditions in different locations, this model cannot be used globally. In 2004, Axel von Engeln calculated the probability of duct anomaly occurrence, the altitudes of duct anomalies, the thicknesses of duct anomalies, and the magnitudes of duct anomalies [8]. In some areas, the frequency of duct anomalies was very high, and the duct anomaly heights were less than 2.5 km. The thicknesses of duct anomalies are generally less than 100 m on land and less than 150 m on the coastline. In 2016, Samer Khanafseh calculated the largest duct anomaly of 30 mm using ERA-Interim 2000-2014 data [9]. In 2018, Beihang University used ERA5 2010-2017 data to calculate duct anomalies in China, and the maximum duct anomaly error in the zenith direction was 45.64 mm. Moreover, it was found that duct anomalies and non-nominal anomalies occur at the same time [10].

This paper studies tropospheric anomalies and overbounded tropospheric

anomaly delays. Section 2 defines tropospheric anomalies, explains the causes of tropospheric anomalies, and illustrates the method of calculating tropospheric delays. Section 3 studies the frequency of non-nominal anomalies and the simultaneous occurrence of the two types of anomalies and simultaneously calculates the maximum residual tropospheric delay caused by non-nominal anomalies and the maximum residual tropospheric delay caused by the simultaneous occurrence of the two types of anomalies. Section 4 studies the impact of tropospheric anomalies on GBAS integrity. The final section provides a summary and outlines future research directions.

2. TROPOSPHERIC ANOMALIES

Tropospheric anomalies mean that tropospheric delays cannot be differentiated or do not match the model under abnormal atmospheric conditions such as weather fronts, heavy rainfall, and temperature inversion. Tropospheric anomalies are divided into those in the horizontal and vertical directions, which are called non-nominal anomalies and duct anomalies, respectively.

2.1 Non-nominal anomalies

Non-nominal anomalies are the tropospheric gradient in the horizontal direction relative to an approaching aircraft. Non-nominal anomalies refer to atmospheric conditions when satellite signals arrive at airborne terminals and are different from those when satellite signals arrive at GBAS stations. Tropospheric delay cannot be eliminated by the differential method. The causes of non-nominal anomalies are weather fronts and heavy rainfall.

There are two kinds of weather fronts: cold fronts and warm fronts. Cold fronts refer to the direction of a cold air mass towards a warm air mass, and warm fronts refer to the direction of a warm air mass towards a cold air mass. The difference in temperature, humidity and air pressure on both sides of the front is very large, and there are often strong winds, rainfall and other atmospheric phenomena. If only the cold and warm peaks are considered, a wedge model can be established. When considering heavy rainfall, the weather wall model can be built [11].

The vertical dotted line in Figure 1 is an infinite vertical wall between the GBAS station and the aircraft assumed by the weather wall model. The atmospheric conditions (temperature, humidity, air pressure) inside (T_w, H_w, and P_w, respectively) and outside (T_0, H_0, and P_0, respectively) the walls are quite different. The path of a satellite signal arriving at the GBAS station is path 2a, path 2b and path 1. The path of a satellite signal arriving at the aircraft is path 3a and path 3b. Under normal atmospheric conditions, the

atmospheric conditions experienced by path 2a, path 3a and path 2b, path 3b are similar, and the tropospheric delay can be eliminated by the difference method. However, under abnormal atmospheric conditions, the atmospheric conditions of path 2b and path 3b are not similar, and the tropospheric delay cannot be eliminated by the difference method. The atmospheric conditions of path 2a and path 3a are very different. If the difference method is used to eliminate the differences, it will yield great difference errors. The difference in the tropospheric delay between path 2a and path 3a is the residual tropospheric delay caused by non-nominal anomalies [12]. There are many ways to calculate the tropospheric delay, such as the Hopfield model and Saastamoinen model [13][14][15][16]. The modified Hopfield model was used to estimate the tropospheric delay in this paper.
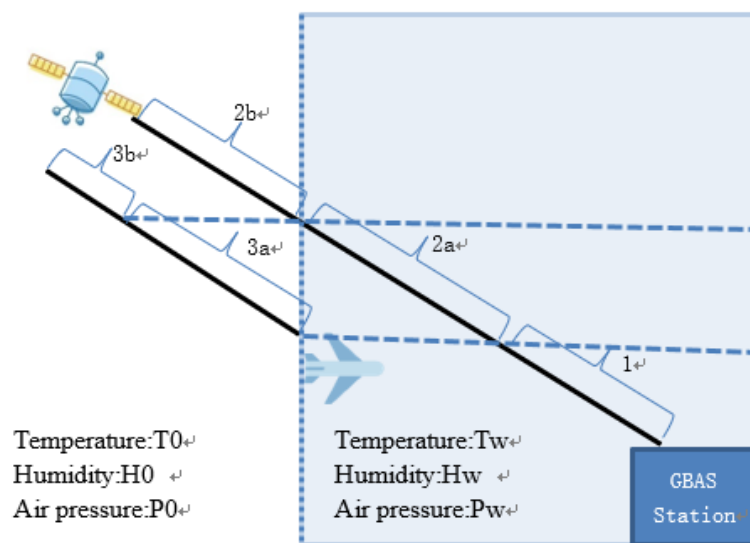
Figure 1 Weather wall model

2.2 Duct anomalies

Duct anomalies refer to the difference between the real gradient of the atmospheric refractive index varying with altitude and the gradient of the atmospheric refractive index as assumed by the TC model, which makes the TC model unable to accurately estimate the tropospheric delay between the GBAS station and airborne terminals. The main factors causing duct abnormalities are the inversion layer and evaporation duct.

The inversion layer is an anomalous phenomenon in which the temperature increases with altitude. Evaporation ducts are phenomena in which the water content in the atmosphere decreases rapidly with altitude. Both anomalous meteorological phenomena will cause gradient anomalies in the refractive index varying with height.

As shown in Figure 1, the duct anomaly occurs in path 1. Under normal conditions, the tropospheric delay calculated by the TC model is not much different from the true tropospheric delay, which can be replaced by the TC

model. However, when atmospheric anomalies occur, the differences between the tropospheric delays calculated by the TC model and the true tropospheric delays are very large, resulting in residual tropospheric delays. A three-parameter model is used to describe duct anomalies. The three-parameter model refers to the height, magnitude and thickness of the duct anomaly. The height of a duct anomaly refers to the height of the beginning of the duct anomaly, the magnitude of a duct anomaly refers to the gradient of the refractive index, and the thickness of a duct anomaly refers to the height of the area where duct anomaly occurs [9].

We use numerical integration to simulate the true tropospheric delays. The difference between the tropospheric delay calculated by the TC model and the true tropospheric delay is the residual tropospheric delay caused by the duct anomaly.

2.3 Data

We used ERA5 data for the calculations. The ERA5 product provides hourly weather data divided into 137 layers, and the highest reachable height is approximately 80 km. The global meteorological data, including temperature, pressure and specific humidity, used in this study are collected from the ECMWF website (https://www.ecmwf.int), which covers the period from 2014 to 2018. The resolution of latitude and longitude is 0.3*0.3, and the sampling rate of the data is 1 hour.

3. STATISTICAL RESULTS

Using the ECMWF data from 2014 to 2018, the frequency of non-nominal anomalies in different regions and seasons and the frequency of duct and non-nominal anomalies in different regions and seasons were analyzed. Moreover, the maximum residual tropospheric delay caused by non-nominal anomalies and the maximum residual tropospheric delay caused by the simultaneous occurrence of duct and non-nominal anomalies are calculated. Finally, the frequency of residual tropospheric delays caused by non-nominal anomalies and the frequency of residual tropospheric delays caused by the simultaneous occurrence of duct and non-nominal anomalies are calculated.

3.1 Non-nominal anomalies

According to Figures 2-5, we can draw the following conclusions: 1) The frequency of residual tropospheric delays exceeding 5 cm caused by non-nominal anomalies is related to the topography. The high frequency places are the Cordillera Mountains in North America, the Andes in South

America, the East African Plateau in Africa, the Iranian Plateau and the Himalayas in Asia, and the islands between Asia and Oceania. 2) The places where a high frequency of residual tropospheric delay caused by non-nominal anomalies greater than 10 cm are the Andes in South America, the Himalayas in Asia, the Iranian Plateau in Asia, the Cordillera Mountains in North America, and the East African Plateau in Africa. 3) The places where a high frequency of residual tropospheric delay caused by non-nominal anomalies greater than 15 cm are the Andes of South America and the Himalayas of Asia. 4) There is almost no place where the residual tropospheric delay caused by non-nominal anomalies exceeds 20 cm.
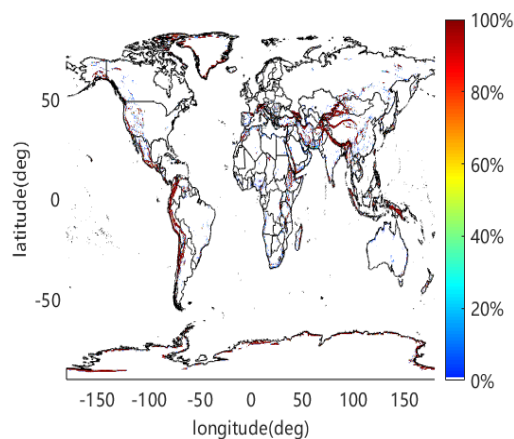
Figure 2 Frequency of residual tropospheric delays greater than 5 cm
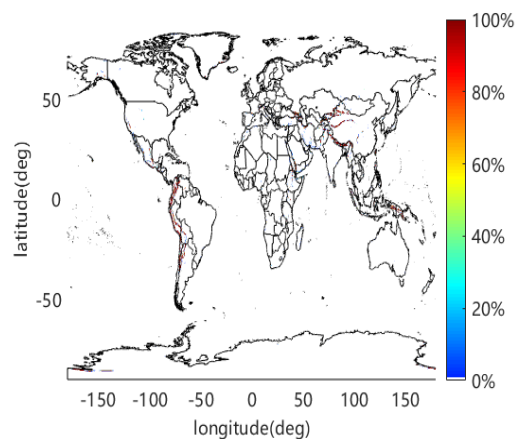
Figure 3 Frequency of residual tropospheric delays greater than 10 cm
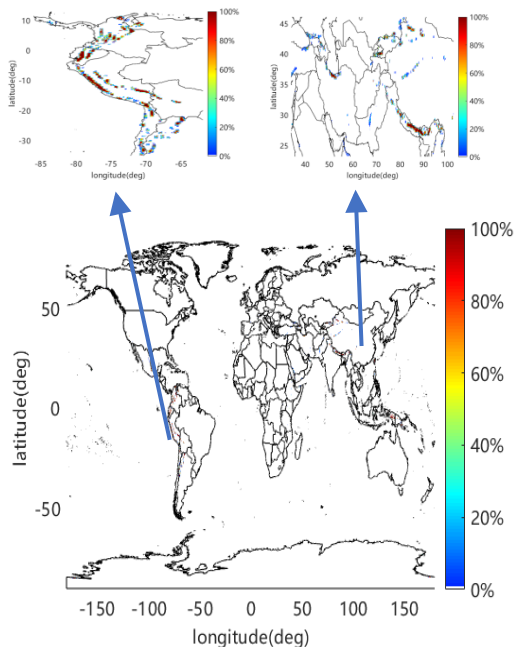
Figure 4 Frequency of residual tropospheric delays greater than 15 cm
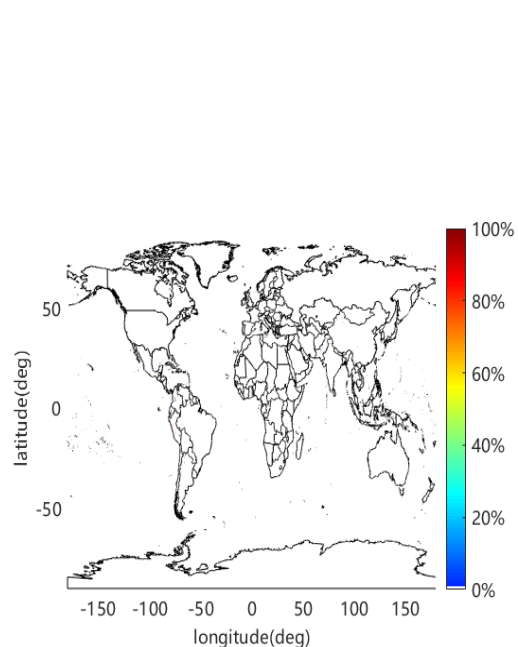
Figure 5 Frequency of residual tropospheric delays greater than 20 cm

As shown in Figure 6, the maximum residual tropospheric delay caused by non-nominal anomalies exceeds 35 cm, and most regions have a residual

tropospheric delay below 15 cm. The maximum residual tropospheric delay caused by non-nominal anomalies is also high where the frequency of non-nominal anomalies is high.
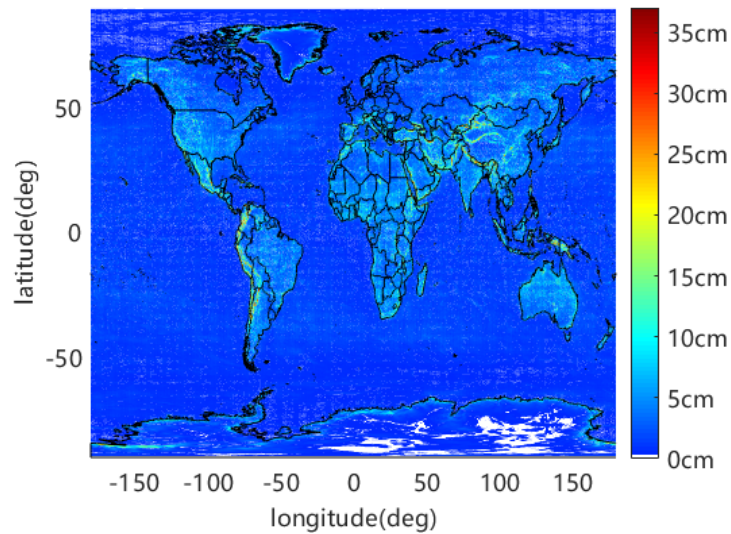
Figure 6 Maximum residual tropospheric delay caused by non-nominal anomalies

As shown in Figures 7-14, the frequencies of residual tropospheric delays exceeding 3 cm caused by non-nominal anomalies in the four seasons of spring, summer, autumn and winter are not very different, and the differences in the maximum residual tropospheric delays caused by non-nominal anomalies in the four seasons are also small. The main reason may be that the important factor affecting the residual tropospheric delays caused by non-nominal anomalies is the topography, and the topography does not change with the seasons.
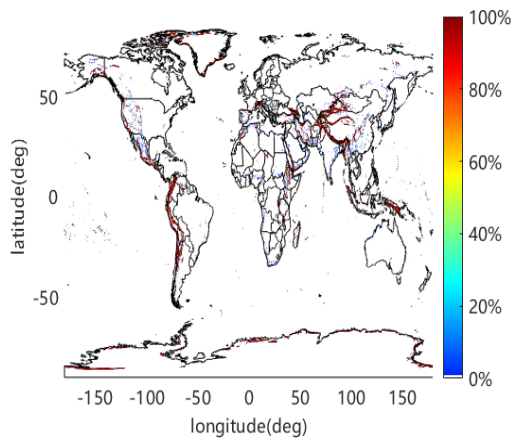
Figure 7 Frequency of non-nominal anomalies in spring
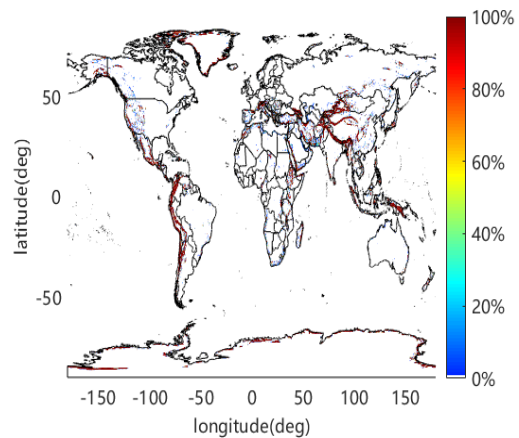
Figure 8 Frequency of non-nominal anomalies in summer
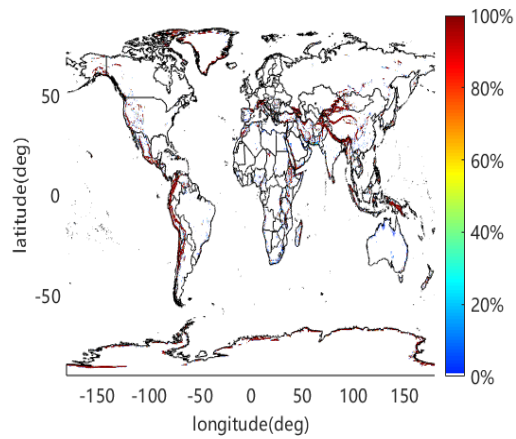
Figure 9 Frequency of non-nominal anomalies in autumn
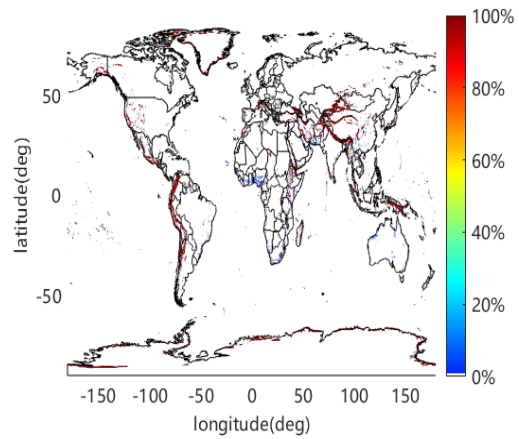
Figure 10 Frequency of non-nominal anomalies in winter
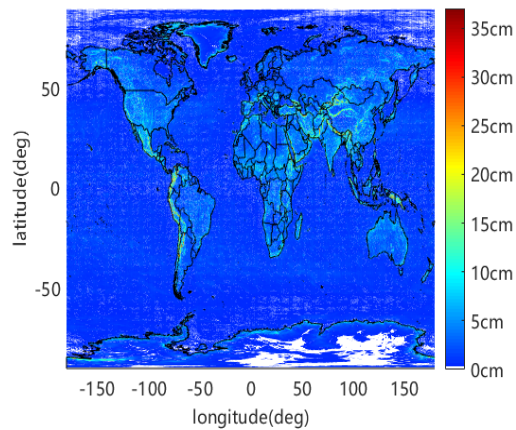

Figure 11 Maximum residual tropospheric delays caused by non-nominal anomalies in spring
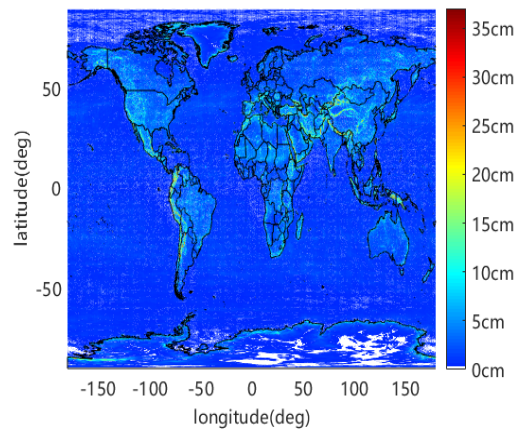

Figure 12 Maximum residual tropospheric delays caused by non-nominal anomalies in summer
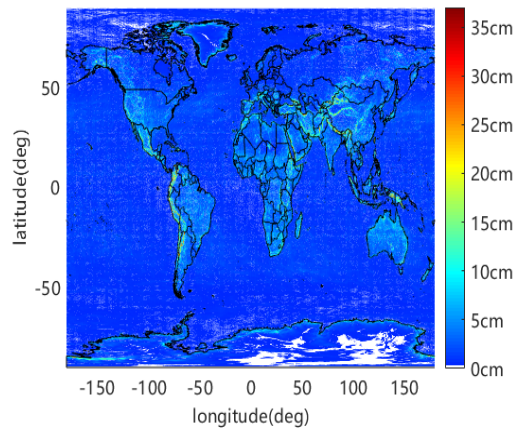
Figure 13 Maximum residual tropospheric delays caused by non-nominal anomalies in autumn
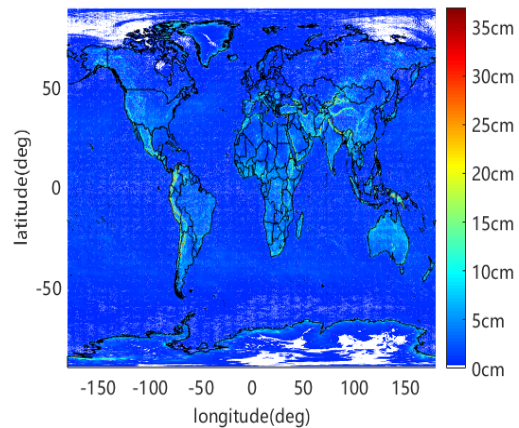

Figure 14 Maximum residual tropospheric delays caused by non-nominal anomalies in winter

As shown in Figure 15, we plotted the frequency histogram of the residual tropospheric delays caused by non-nominal anomalies. The residual tropospheric delays caused by non-nominal anomalies are mostly less than 5 cm, and the frequency is over 90%.
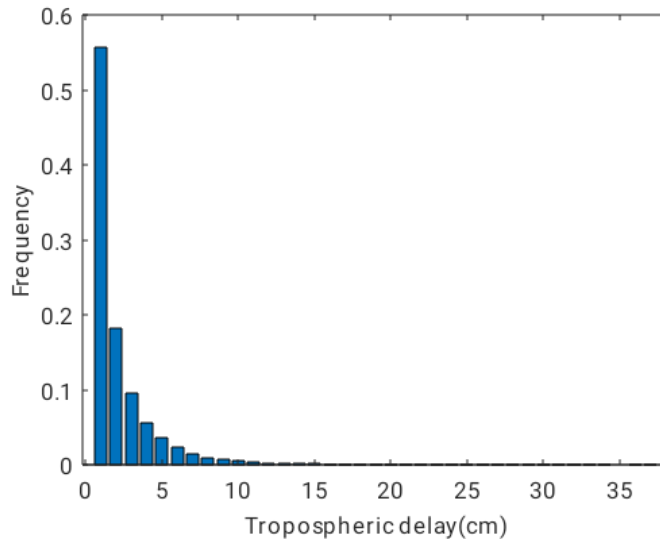
Figure 15 Residual tropospheric delay histogram caused by non-nominal anomalies

3.2 Duct anomalies and non-nominal anomalies

As shown in Figure 16, we can draw the following conclusions: 1) Non-nominal anomalies and duct anomalies occur frequently in coastal areas, and the frequency of duct anomalies and non-nominal anomalies near the Himalayas is relatively low, which is different from the frequency of non-nominal anomalies. 2) The maximum frequency of duct and non-nominal anomalies occurring simultaneously is 70%. 3) There is a high frequency of two anomalies in the Mediterranean Sea, the Red Sea, the Black Sea, the Arabian Sea, etc.
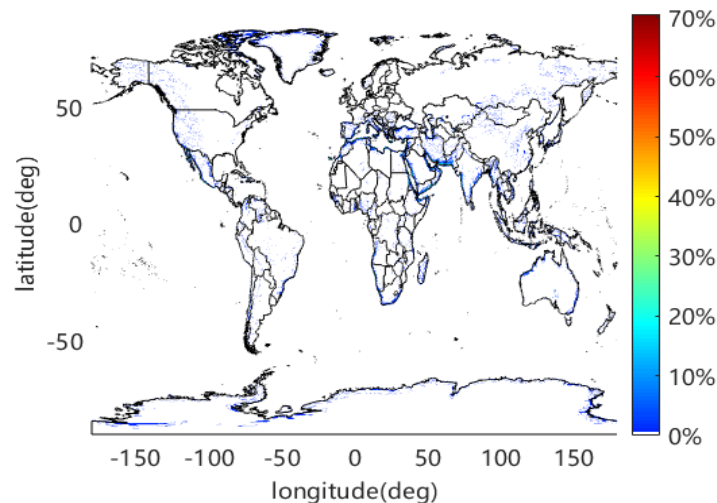

Figure 16 Frequency of duct anomalies and non-nominal anomalies

As shown in Figures 17-20, we can see that different seasons have different frequencies of the simultaneous occurrence of duct and non-nominal anomalies. Among them, the first is summer, the maximum frequency of the two kinds of anomalies occurring at the same time is 98.81%, and there are

more areas where the two kinds of anomalies occur frequently in the four seasons. The second is spring, the maximum frequency of the types of two anomalies occurring simultaneously is 90.81%, and the third is autumn, the maximum frequency of the two kinds of anomalies occurring simultaneously is 61.20%. Finally, it is winter, and the maximum frequency of the two types of anomalies occurring simultaneously is 52.78%.
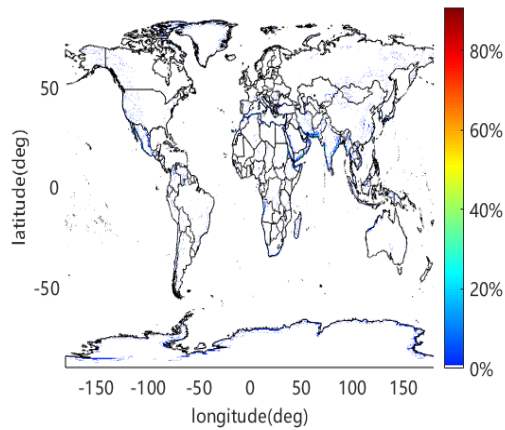

Figure 17 Frequency of duct anomalies and non-nominal anomalies in spring
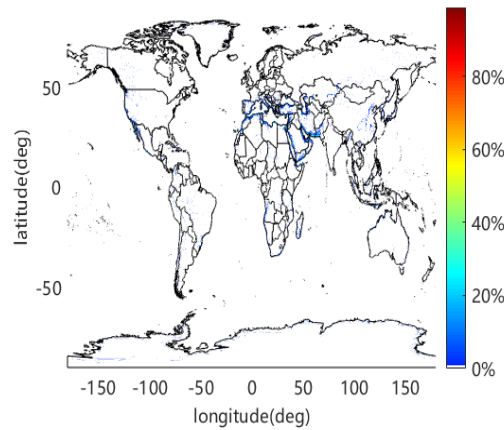

Figure 18 Frequency of duct anomalies and non-nominal anomalies in summer
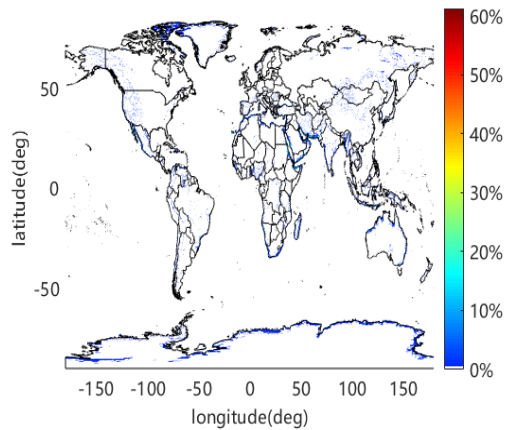
Figure 19 Frequency of duct anomalies and non-nominal anomalies in autumn
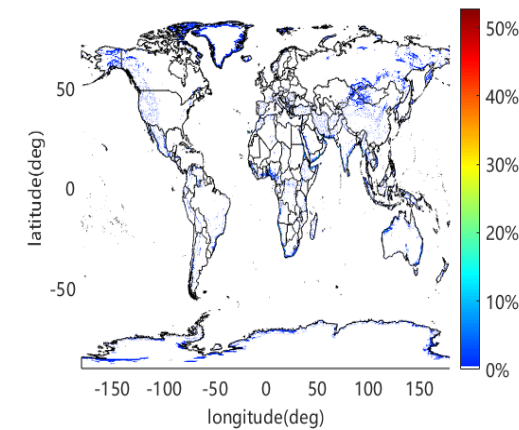

Figure 20 Frequency of duct anomalies and non-nominal anomalies in winter

As shown in Figures 21-25, we can see that residual tropospheric delays caused by the two types of anomalies are similar to those caused by non-nominal anomalies. The reason is because non-nominal anomalies are dominant when the two kinds of anomalies occur simultaneously. The maximum residual tropospheric delay caused by non-nominal anomalies is 36.0639 cm in spring, 35.6443 cm in summer, 34.7294 cm in autumn and 34.0492 cm in winter. The maximum residual tropospheric delay caused by duct and non-nominal anomalies is 36.1128 cm in spring, 35.6981 cm in summer, 34.7734 cm in autumn, 34.1040 cm in winter.
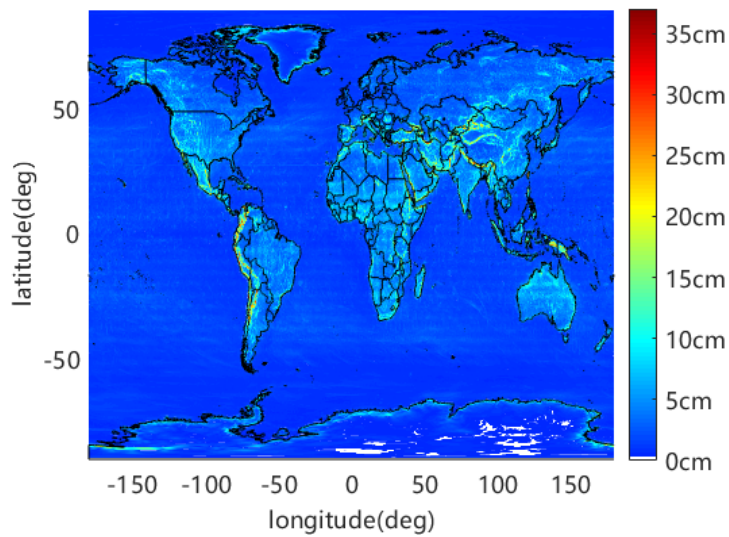
Figure 21 Maximum residual tropospheric delays caused by duct and non-nominal anomalies
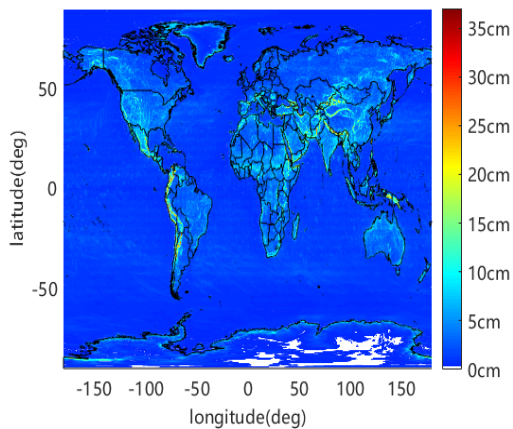

Figure 22 Maximum residual tropospheric delays caused by duct and non-nominal anomalies in spring
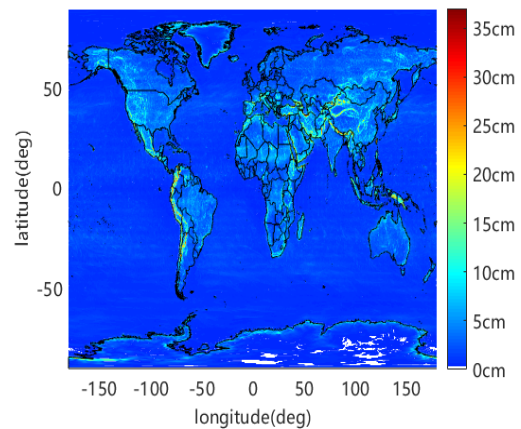

Figure 23 Maximum residual tropospheric delays caused by duct and non-nominal anomalies in summer
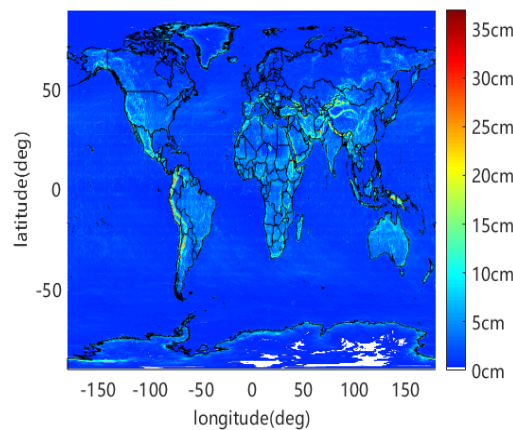

Figure 24 Maximum residual tropospheric delays caused by duct and non-nominal anomalies in autumn
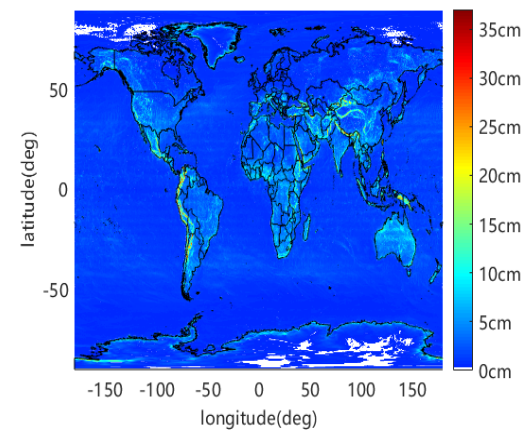

Figure 25 Maximum residual tropospheric delays caused by duct and non-nominal anomalies in winter

As shown in Figure 26, the residual tropospheric delays caused by the

simultaneous occurrence of duct and non-nominal anomalies are mostly less than 5 cm, the residual tropospheric delays caused by the simultaneous occurrence of the two types of anomalies are mostly 2 cm, but the residual tropospheric delays caused by non-nominal anomalies are mostly 1 cm. This finding shows the effect of duct anomalies on the residual tropospheric delays.
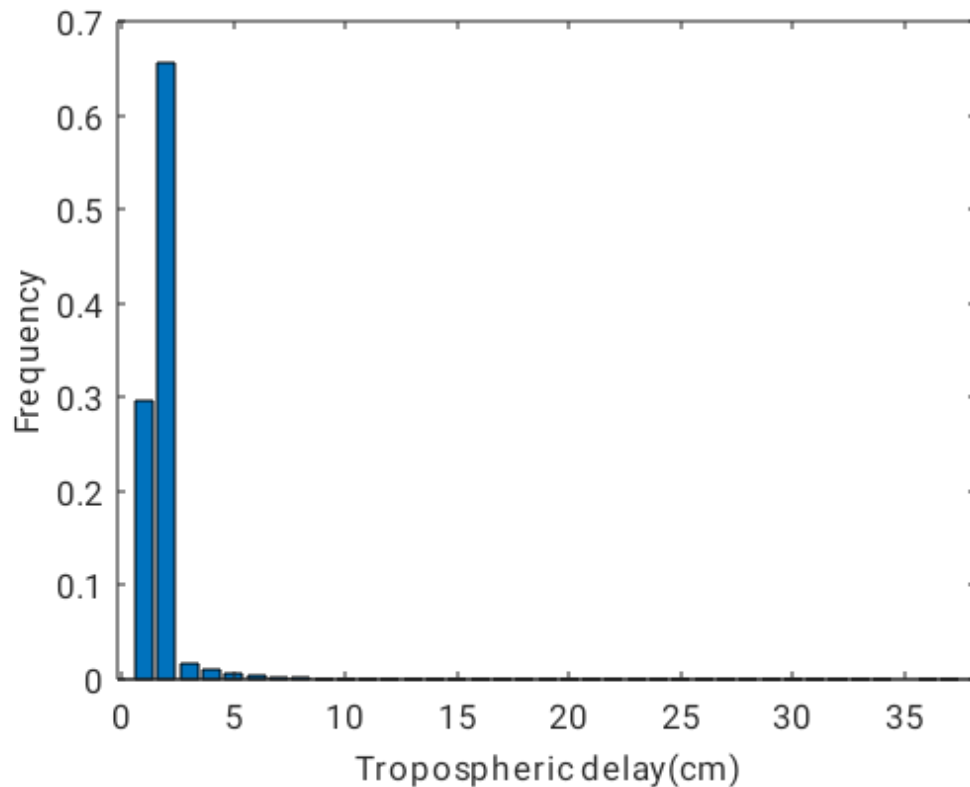

Figure 26 Residual tropospheric delay histogram caused by the duct and non-nominal anomalies

4. ANOMALOUS TROPOSPHERE BOUNDING

When anomalous atmospheric conditions occur, they will affect the positioning accuracy of the aircraft, causing miss alarms during aircraft approach. Therefore, it is necessary to add this bias to the calculation of the protection level. Previous scholars have studied the overbound method for the residual troposphere delay [17]. The maximum residual tropospheric delay caused by the duct anomaly is proposed as the overbound value for the duct anomaly, and the mathematical model is obtained by overbounding the residual tropospheric delay caused by non-nominal anomalies. However, the mathematical model established by previous scholars relies only on the IGS and iGMAS station data [5]. It is too conservative and not applicable to the area where a GBAS station is located. We use the grid data to establish the residual tropospheric delay mathematical model caused by non-nominal anomalies and analyze the impact of new modeling methods on the

protection level at Dongying Airport.

4.1 Mathematical model for non-nominal anomalies

The previous method calculates the residual tropospheric delay using the projection function method. In this paper, we use grid data to calculate residual tropospheric delays at different elevation angles and establish mathematical models. The specific steps are as follows:

1) because the height layers are not equally spaced, it is necessary to interpolate the meteorological data in the vertical direction so that the height layers are equally spaced.
2) the differential tropospheric delay between two adjacent points is calculated.
3) the tangent of the elevation angle is calculated.
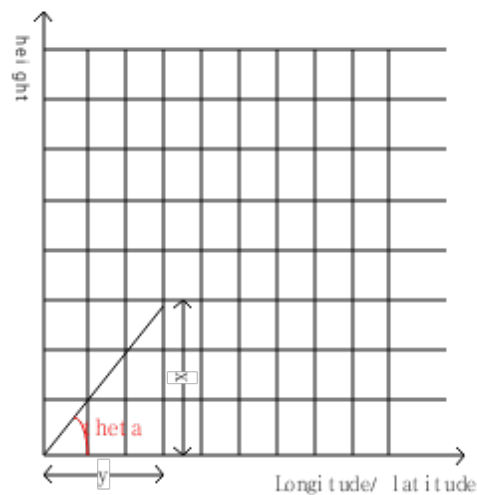
Figure 27 Calculation of the tangent of the elevation angle

$$\tan \theta = \frac{x}{y} \qquad (1)$$

$$Elevation = \tan^{-1} \frac{x}{y} \qquad (2)$$

4) the residual tropospheric delay at different elevation angles is calculated by numerical integration.
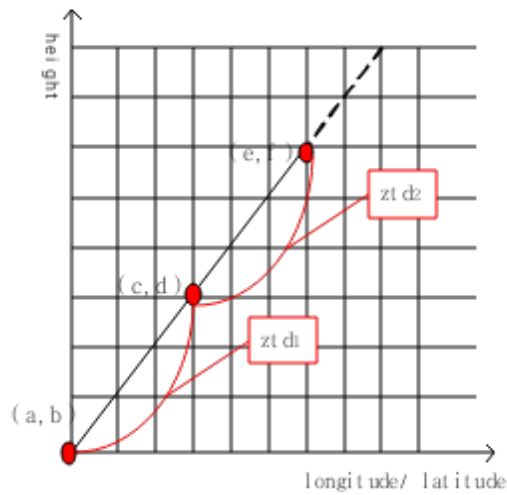
Figure 28 uses grid data to calculate the tropospheric delay

$$ZTD = ztd_1 + ztd_2 + \cdots \qquad (3)$$

$$ztd_1 = ztd_{(c,d)} - ztd_{(a,b)} \qquad (4)$$

$$ztd_2 = ztd_{(e,f)} - ztd_{(c,d)} \qquad (5)$$

where $ztd_{(e,f)}$ is calculated using the modified Hopfield model.

5) the maximum residual tropospheric delays in both directions are found

This paper calculates the residual tropospheric delay caused by non-nominal anomalies using the data from May 10, 2018, downloaded from the ECMWF website, and the resolution of latitude and longitude is 0.125*0.125. The results are as follows.

Table 1 Residual tropospheric delays at different elevations

Elevation (degrees)	0.0139	0.0208	0.0417	1.4026	2.1034	2.7897	4.1735	4.1804
ZTD (m)	0.0992	0.0987	0.0971	0.0418	0.0313	0.0249	0.0177	0.0176
Elevation (degrees)	4.2011	5.5524	6.2464	6.9249	8.2895	8.2963	8.3167	9.6447
ZTD (m)	0.0176	0.0137	0.0123	0.0112	0.0094	0.0094	0.0094	0.0082
Elevation (degrees)	10.3250	10.9890	12.3213	12.3279	12.3478	13.6401	14.3007	14.9444

ZTD (m)	0.0077	0.0072	0.0065	0.0065	0.0065	0.0059	0.0056	0.0054
Elevation (degrees)	16.2330	16.2394	16.2586	17.5050	18.1407	18.7594	19.9954	20.00154
ZTD (m)	0.0050	0.0050	0.0050	0.0046	0.0045	0.0043	0.0041	0.0041
Elevation (degrees)	20.0199	21.2123	21.8194	22.4095	23.5864	23.5922	23.6097	24.7425
ZTD (m)	0.0041	0.0039	0.0038	0.0037	0.0035	0.0035	0.0035	0.0033
Elevation (degrees)	25.3184	25.8776	26.9913	26.9968	27.0133	28.0833	28.6265	29.1536
ZTD (m)	0.0033	0.0032	0.0031	0.0031	0.0031	0.0030	0.0029	0.0029
Elevation (degrees)	30.2020	30.2072	30.2227	31.2286	31.7387	32.2333	33.2163	33.2212
ZTD (m)	0.0028	0.0028	0.0028	0.0027	0.0027	0.0026	0.0026	0.0026
Elevation (degrees)	33.2357	34.1777	34.6551	36.0410	36.0546	37.37980	38.67250	38.68520
ZTD (m)	0.0026	0.0025	0.0025	0.0024	0.0024	0.0023	0.0022	0.0022
Elevation (degrees)	39.9201	41.1239	41.1357	42.2851	43.4050	43.4160	44.4850	45.5264
ZTD (m)	0.0022	0.0021	0.0021	0.0021	0.0020	0.0020	0.0020	0.0020
Elevation (degrees)	45.5366	47.5086	49.3428	51.0497	52.6395	54.1217	55.5048	56.7972
ZTD (m)	0.0020	0.0019	0.0018	0.0018	0.0018	0.0017	0.0017	0.0017

Elevation (degrees)	58.0063	59.1389	60.2012	61.1989	62.1372	63.0207	63.8538	
ZTD (m)	0.0017	0.0016	0.0016	0.0016	0.0016	0.0016	0.0016	

We establish a mathematical model based on the data in the above table.
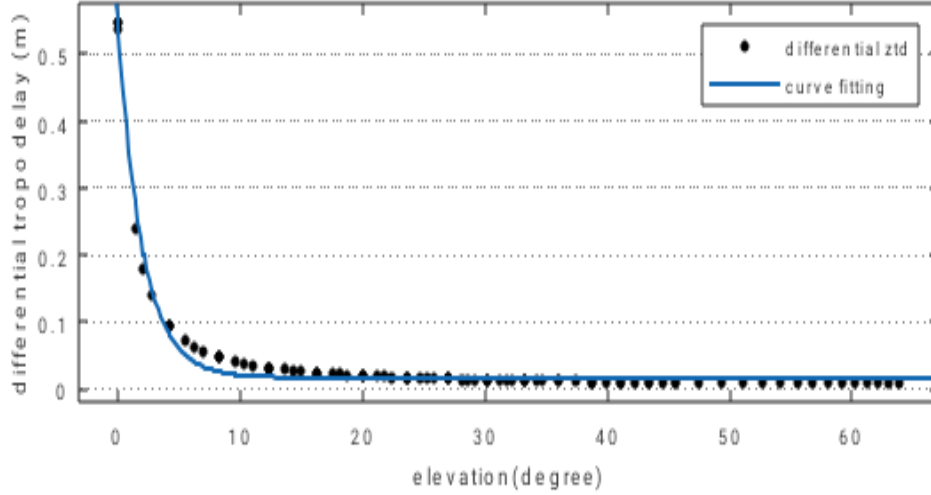
Figure 29 Curve based on the data in the above table

Table 2 Mathematical model based on the data in the above table

General model	Coefficients (with 95% confidence bounds)	SSE	R squared	RMSE
f(x)=a*exp(-b*x)+c	a= 0.5264 (0.5139, 0.539) b=0.4975 (0.4697, 0.5254) c=0.01695 (0.01447, 0.01942)	0.0097	0.9891	0.0107

4.2 Protection Level

In 2004, Frank Van Graas et al. proposed the calculation method of ideal VPL [18]. This calculation method divides the protection level into two parts: the protection level under normal conditions and the protection level under anomalous conditions.

$$VPL = VPL_{normal} + VPL_{bias} \qquad (6)$$

For duct anomalies, the maximum value of the residual tropospheric delay caused by duct anomalies over time is used as the overbound value.

$$VPL_{bias\_duct} = \sum_{i=1}^{N} \left| S_{v,i} u_{duct,max} \right| \qquad (7)$$

N is the number of ranging sources used in the position solution.

S is the projection matrix that relates the range domain measurements to the position domain estimates.

For non-nominal anomalies, the results calculated using the established mathematical model are overbounded as overbound values.

$$VPL_{bias\_non} = \sum_{i=1}^{N} \left| S_{v,i} u_{non,max} \right| \qquad (8)$$

$$u_{non,max} = 0 \cdot 5264 * \exp\left(-0.4975*\theta\right) + 0 \cdot 01695 \qquad (9)$$

where θ is the elevation angle.

We compare the impact of the two anomalies on the protection level. The specific results are shown below.
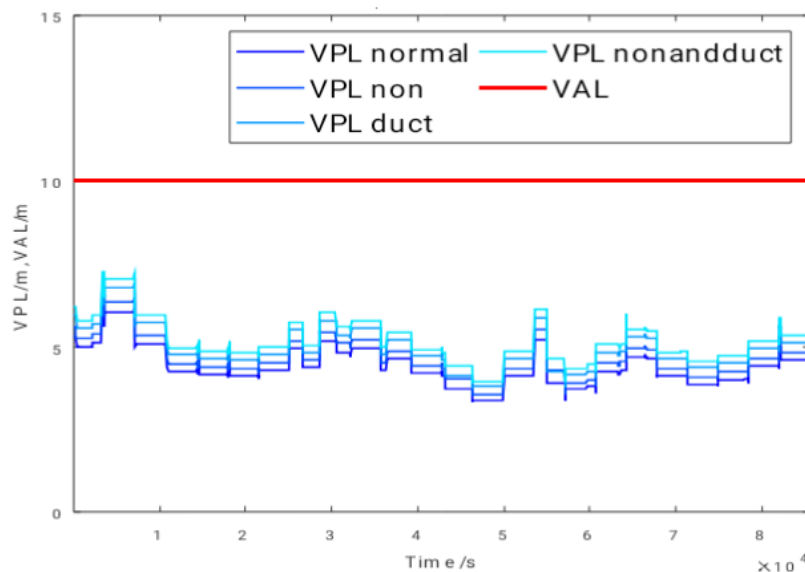

Figure 30 Vertical protection level

As shown in Figure 30, at Dongying Airport, the influence of duct anomalies on the protection level is greater than that of non-nominal anomalies. Among them, duct abnormalities will increase the protection level by 0.9246 m, and non-nominal abnormalities will increase the protection level by 0.2444 m. The simultaneous occurrence of the two types of anomalies will increase the protection level by 1.1303 m.

5. SUMMARY

We analyzed the frequency of non-nominal anomalies in different seasons and the maximum residual tropospheric delays caused by non-nominal anomalies in different seasons and in different regions. Moreover, the frequency of non-nominal and duct anomalies in different seasons and the maximum residual tropospheric delay caused by non-nominal and duct anomalies in different seasons are analyzed. The residual tropospheric delay caused by non-nominal anomalies exceeds 35 cm in some areas. The main

factor found to affect non-nominal anomalies is the topography.

We analyzed the impact of duct anomalies and non-nominal anomalies on the protection level of the GBAS near Dongying Airport, and found that duct anomalies have a greater impact on Dongying Airport than non-nominal anomalies.

ACKNOWLEDGMENTS

REFERENCES

[1]"RTCA DO-245A. minimum aviation system performance standards for the local area augmentation system (LAAS).

[2] Alexander, K. et al., WP16, ICAO NSP/WGW, May 2014.

[3] Guilbert, Alizé, "Non-Nominal Troposphere Reassessment for Meeting CAT II/III with MC/MF GBAS," Proceedings of the 28th International Technical Meeting of the Satellite Division of The Institute of Navigation (ION GNSS+ 2015), Tampa, Florida, September 2015.

[4] Huang,J.,Van Graas,F.,and Cohenour,C..Characterization of Tropospheric Spatial Decorrelation Errors Over a 5-km Baseline. NAVIGATION:Journal of The Institute of Navigation,Spring 2008.

[5] Huang,J.,and Van Graas,F.. Comparison of Tropospheric Decorrelation Errors in the Presence of Sever Weather Conditions in Different Areas and Over Different Baseline Lengths[J].NAVIGATION:Journal of The Institute of Navigation,Fall 2007.

[6] Wang, Zhipeng & Xin, Pumin & Li, Rui & Wang, Shujing. A Method to Reduce Non-Nominal Troposphere Error. Sensors (Basel, Switzerland),2017.

[7] Yoshihara, Takayuki, Saito, Susumu, Kezuka, Atsushi, Saitoh, Shinji, "Revaluation of Spatial Decorrelation Parameters of Atmospheric Delay for GBAS (Ground-based Augmentation System) Safety Design," Proceedings of the ION 2019 Pacific PNT Meeting, Honolulu, Hawaii, April 2019.

[8] Von Engeln A, Teixeira J. A ducting climatology derived from the European Centre for

Medium-Range Weather Forecasts global analysis fields. Journal of Geophysical Research, 2004.

[9] Samer Khanafseh, Boris Pervan and Axel Von Engeln, "Tropospheric Duct Anomaly Threat Model for High Integrity and High Accuracy Navigation" Proceedings of ION GNSS+ 2016, Portland, OR, Sept.12-16,2016.

[10] Zhang, Yue & Wang, Zhipeng.. The Impact of Tropospheric Anomalies on Sea-Based JPALS Integrity. Sensors,2018.

[11] van Graas, F., Zhu, Z., "Tropospheric Delay Threats for the Ground Based Augmentation System," *Proceedings of the 2011 International Technical Meeting of The Institute of Navigation*, San Diego, CA, January 2011.

[12] Guilbert, Alizé, Milner, Carl, Macabiau, Christophe, "Characterization of Tropospheric Gradients for the Ground-Based Augmentation System Through the Use of Numerical Weather Models", *NAVIGATION, Journal of The Institute of Navigation*, Vol. 64, No. 4, Winter 2017.

[13] Hopfield H S. Two- quartic troposphere refractivity profile for correcting satellite data. Journal of Geophysical Research, 1969.

[14] Saastamoinen J. Contributions to the theory of atmospheric refraction. Bulletin Géodésique, 1972.

[15] Tunalı, Engin & Ozludemir, M.. . GNSS PPP with different troposphere models during severe weather conditions. GPS Solutions,2019.

[16] Narayanan, Shrivathsan, Osechas, Okuary, Günther, Christoph, "Tropospheric Delays for Ground-to-Air Radio Links," Proceedings of the 2017 International Technical Meeting of The Institute of Navigation, Monterey, California, January 2017.

[17] Guilbert, Alizé, Milner, Carl, Macabiau, Christophe, "Troposphere Reassessment in the scope of MC/MF Ground Based Augmentation System (GBAS)," Proceedings of the ION 2015 Pacific PNT Meeting, Honolulu, Hawaii, April 2015.

[18] F. van Graas, V. Krishnan, R. Suddapalli, T.Skidmore, Conspiring Biases in the Local Area Augmentation System, Proceedings of ION Annual Meeting 2004.